PREDICTION OF ISOTACHOPHORESIS STEADY-STATE ZONE POSITION AND ANALYSIS OF ZONE BEHAVIOR AROUND A 180° TURN

By

SCHURIE LANETTE MOREAU HARRISON

A thesis submitted in partial fulfillment of
the requirements for the degree of

MASTER OF SCIENCE IN CHEMICAL ENGINEERING

WASHINGTON STATE UNIVERSITY
Department of Chemical Engineering

AUGUST 2007

To the Faculty of Washington State University:

The members of the Committee appointed to examine the thesis of SCHURIE LANETTE MOREAU HARRISON find it satisfactory and recommend that it be accepted.

_____

Chair

_____

_____

ACKNOWLEDGEMENTS

I would like to thank my advisor, Dr. Ivory for all of his support and faith in my research. I would also like to thank him for all of the paper editing, especially at the end when it was time to get everything finished up. I would also like to thank the Ivory lab group, for all of their input and ideas on my research. Thanks to all of you for bringing up questions that I hadn't thought of.

Additionally, I would like to thank my committee Dr. Ha and Dr. Van Wie. Dr. Ha, thank you for offering your help to me at anytime. Dr. Van Wie, your guidance at the beginning of my career made writing my thesis introduction go by smoothly and saved me a lot of time when I needed it most.

Diana Thornton, JoAnn McCabe, and Senja Estes, thank you. Your help is invaluable. Diana, thank you for your willingness to figure out all of the problems I encounter with scheduling, getting paid, and other administrative issues. Additionally, your humor is always appreciated… as long as I know you are kidding. JoAnn, thank you for always getting my orders out even though I rarely came to you with a budget number ready. Senja, I appreciate your advice on any issue, whether working the copy machine, or fixing dinners.

Finally, I would like to thank my family and friends, who have pushed me to continue my education. They have also provided the emotional support and encouragement needed during my graduate studies.

PREDICTION OF ISOTACHOPHORESIS STEADY-STATE ZONE POSITION AND ANALYSIS OF ZONE BEHAVIOR AROUND A 180° TURN

Abstract

by Schurie Lanette Moreau Harrison, M.S.

Washington State University

August 2007

Chair: Cornelius F. Ivory

Isotachophoresis (ITP) has the ability to both concentrate and purify analytes, and thus is a candidate for the purification of low abundance species found in many systems, including human blood serum. In this thesis, the theory and background of ITP is presented followed by two novel articles prepared for submission to scientific journals.

The first article develops an analytical expression to predict the location of stationary steady-state ITP zones. Theoretical zone position predictions were compared to experimental results obtained using a vortex stabilized electrophoresis apparatus. The analytical model was found to predict all experimental zone positions within the 95% confidence interval of the data.

The second article presents a 2-D simulation of ITP in two turn, or S channel. The introduction of turns into a channel provides two sources of dispersion, both from the

difference in electric field strength, and distance a zone must travel across the width of the channel. The simulation presented shows that ITP zones are able to recover from the dispersion introduced by the turns in a straight segment following the turn. The effects of turn radius, voltage and sample mass on the length of straight segment required for zone recovery are presented.

TABLE OF CONTENTS

LIST OF TABLES

LIST OF FIGURES

DEDICATION

This thesis is dedicated to my father, mother, sisters, brothers and husband. I love you all.

CHAPTER ONE

INTRODUCTION

The human proteomics initiative (HPI) is the task of providing for each known protein a description of its function, domain structure, subcellular location, post-translational modifications, variants, and any other information known [1]. Using this information new disease markers and drug targets may be identified to help prevent, diagnose and treat disease. For example, the serious liver pathology of cirrhosis can be detected by a decline in the net amounts of the proteins, haptoglobin and albumin, and inflammation or infection can be detected by measuring levels of interleukin-6 [2]. The normal concentrations of albumin and interleukin-6 are 35-50 mg/ml and 0-5 pg/ml, respectively. Thus, the concentrations of these two clinically valuable proteins differ by a factor of 10^{10}. Methods currently available for the discovery of novel proteins, such as two-dimensional electrophoresis and mass spectrometry, have a dynamic range of only 10^2 to 10^4 [2]. Therefore, there is a need for improved methods of purifying proteins, particularly when there are species of very low concentration in the solute relative to other species.

In this work, the electrophoretic method known as isotachophoresis (ITP) is explored due to its unique characteristic of both concentrating and separating proteins. Due to these characteristics, it is proposed that ITP will be a suitable method for purifying proteins, which may otherwise be in undetectable low concentrations due to the surrounding high abundance proteins that interfere

with recognition. This chapter will cover previous work on ITP theory and modeling, compare ITP to other electrophoretic purification techniques, and introduce the theory of multi-scale ITP.

Chapter two, a paper prepared for submission to *Journal of Separation Science*, derives an analytical expression for predicting the position of immobilized ITP zones as a function of current. Comparison to experimental results obtained in a preparative scale apparatus at WSU showed that the model was able to predict zone location with reasonable accuracy. In chapter three, the results of a 2-D simulation of ITP using COMSOL Multiphysics v 3.3 are presented. This simulation studies the behavior of ITP zones following a pair of 180° turns. Simulation results, as well as experimental observations from ITP in an S channel, are presented in a paper formatted for submission to *Electrophoresis*.

1.1 Theory and Modeling

Electrophoresis is the separation of charged particles in response to an applied electric field. Under the influence of an electric field, cations will migrate towards the cathode, and anions will migrate towards the anode. In ITP, a discontinuous buffer system is used, where sample is injected between a leading and terminating electrolyte having the highest and lowest mobility, respectively, of all of the sample species. With applied current, individual species with the same charge sign are ordered according to their electrophoretic mobility in adjacent, self sharpening zones. All species with the same charge sign move with equal velocity at *pseudo* steady-state. The concentration of zones is dependent on the concentration of the leading electrolyte, allowing for both concentration and separation of species to occur. With sufficient mass of sample, a

plateau concentration is attained once the ITP zones have reached *pseudo* steady-state. This concentration is described by the following equation [3]:

$$\frac{c_j}{c_{LE}} = \frac{z_{LE}(\mu_{LE} - \mu_m)\mu_j}{z_j(\mu_j - \mu_m)\mu_{LE}},$$

where μ_i is the electrophoretic mobility, c_i the concentration, and z_i the charge of the i^{th} component. The subscripts LE, j and m represent the leading electrolyte, sample species, and counterion, respectively.

According to a review on ITP written in 1991, the focus of theoretical research was on computer simulation projects. In the past decade, PC's have become ubiquitous, allowing for computer modeling to be conducted in every laboratory [4]. Early computer simulations showed pH dips at zone boundaries, however by 2002, improved models were presented [5]. By applying a flux-corrected transport finite difference method to the transient one-dimensional model, it was shown that pH dips reported were an artifact of the numerical methods used [5].

In 1995, Gebauer *et al.* published a paper on the theory of ITP taking a diffusional approach [6]. This model helps explain the boundary layer between two adjacent bands, by addressing the dispersive forces that introduce overlap between the bands. This theory is critical to understanding the resolution of a particular species, where resolution is defined as the ratio of the amount of a species which is pure to the total amount of that species. According to Gebauer *et al.* the highest resolution is achieved when the sum of the sample zone lengths equals the

selectivity multiplied by the length of the separation column, where selectivity is defined as the relative mobility differences between two species.

To illustrate the resolution that can be obtained using ITP, consider two species with high selectivity, or a large difference in mobilities. The self-sharpening effect at the boundary between the two zones is strong, and results in a negligible overlap between the adjacent species. Thus for long sample zones the resulting resolution is effectively unity. For a species pair with low selectivity, however, the self sharpening properties of the zone boundary are poor. This results in a greater overlap between adjacent zones, consequently giving poorer resolution. This leads to the separation limitation of ITP, which occurs when the selectivity is so low that sufficient resolution is unattainable [6]. However, Karel Šlais introduced a model which showed that the overlap between adjacent bands decreases in a tapered capillary [7], therefore improving resolution. Šlais noted that it is advantageous to couple ITP in a large cross section into a smaller cross section. The larger cross section is used as a pre-concentration step, while the narrow channel is used for the detection of longer zones. Figure 1.1 illustrates the longer zones obtained when moving from a larger to smaller cross-sectional area.

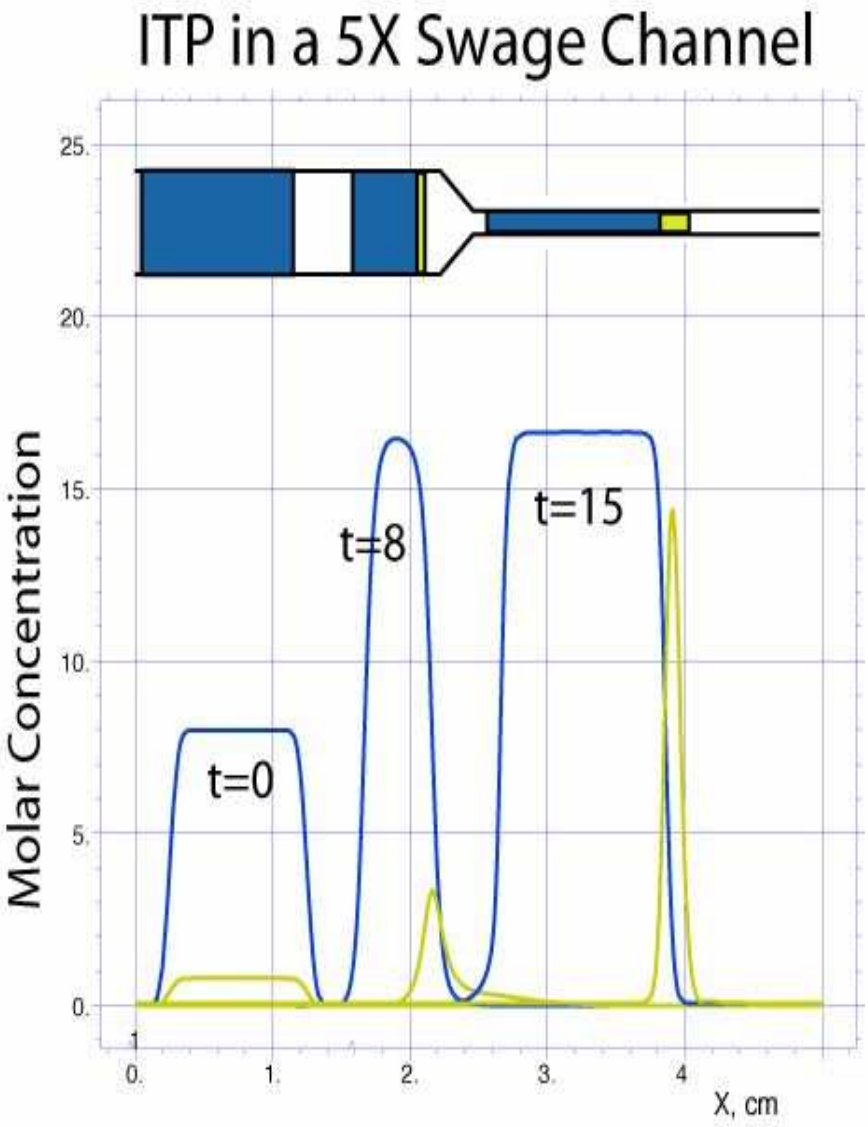

Figure 1.1: Simulation of a two component sample with a 10x mass difference undergoing ITP through a 5x reducing or "swage" channel. In the wide portion of the channel the low mass solute moves to the front of the ITP train. After passing into the narrower portion of the channel, the low mass solute increases in both concentration and purity. (Simulation by Cornelius Ivory, WSU)

The present work focuses on the study of ITP zone behavior for the benefit of future studies on multi-scale ITP, or moving from meso to micro scale and lower. In chapter two, an analytical model is presented which allows an experimenter to immobilize an ITP zone at a specific location. One can then remove that sample zone. This can be done batchwise, or continuously. Once a sample has been removed from this scale, it can then be injected into a smaller scale ITP device to enhance purification of zones. In chapter three, ITP in an S channel is explored. This allows for increased channel length on a smaller platform, thus resulting in better resolution of sample zones.

1.2 ITP in Contrast to other Electrophoretic Methods

There are a variety of electrophoretic methods used for purification, including zone electrophoresis (ZE), isoelectric focusing (IEF), and ITP. ZE, like ITP separates samples based on the electrophoretic mobility of a species, while IEF separates based on the isoelectric point of a species. Combinations of ITP, IEF and ZE have also been explored.

Separation via ZE is achieved by the injection of sample into a background electrolyte of a constant composition, pH and conductivity [8]. The use of ZE allows for high separation efficiency and detection sensitivity [4]. This is a gentle separation technique; however its inadequacy lies in the fact that it lacks the ability to concentrate or focus zones. This means that although this separation technique can be employed for very sensitive species, the resulting concentration is equal to or less than the concentration of the species in the original sample, due to diffusion, hydrodynamic dispersion and electroosmotic dispersion, which widen the sample

streams [9]. Due to its non-focusing characteristic, ZE alone is not a suitable separation method for samples containing species that are found in very low concentrations, such as interleukin-6.

In IEF, a pH gradient is formed using a set of carrier ampholytes, which are mixtures of a large number of low molecular weight amphoteric species characterized by slightly different isoelectric points [10]. Species move through the pH gradient until the pH is equal to their isoelectric point (pI), at which point the species has no charge. Once a species reaches its pI it becomes immobile and focused [8]. IEF has the ability to purify proteins with much higher resolution than ZE, however, precipitation or aggregation of many proteins near their pI values creates a definite disadvantage in this environment [9]. In addition, the band sharpening forces of IEF are often not strong enough to overcome the hydrodynamic band broadening effect [9].

Due to the unique characteristic of concentrating and purifying species simultaneously, ITP is frequently used as a pre-separation and pre-concentration step prior to ZE, which has a higher resolving power and sensitivity [11]. Using column-coupling, ITP can be combined on-line with ZE (ITP-ZE) to first concentrate and remove the bulk of other species, before further separation using ZE [12]. In addition, it has been found that sample zones in ITP-ZE are usually sharper than those of ZE due to the fact that there is less dispersion [13]. Krivankova *et al.* reported that using ITP-ZE coupling in capillaries resulted in a 10^3 fold increase in detectability over ZE alone. Additionally, this technique allowed for the determination of species with a concentration ratio of 10^5:1 [13].

Mohan *et al.* studied coupling of IEF with ITP and ZE (IEF-ITP-ZE), which allowed for the discovery of 1,174 proteins for the bacterial species S. *oneidensis* [12]. Their research utilized the separation based on pIs of IEF, followed by ITP and ZE. The rationale behind this method was that species with similar pIs have different electrophoretic mobilities, so by dividing the separated sample from IEF into nine fractions, and subsequently injecting into ITP-ZE, greater separation capabilities may be achieved.

Although coupling of electrophoretic methods has allowed for separation of species with concentration ratios up to 10^5:1, this still falls short of the 10^{10} concentration difference that is found for various species of interest in human plasma [2]. The fact that dilute species are concentrated during the purification process gives ITP a distinct advantage over ZE when studying low concentration proteins. In addition, unlike IEF, ITP zones form based on their electrophoretic mobility, so buffer solutions can be set at a pH that is not close to the pIs of sample proteins. This eliminates the precipitation and aggregation of proteins that often occurs near their pIs.

1.3 ITP Applications

Use of varying sized separation apparatuses allows for a broad set of applications from analytical to preparative scales. At the preparative scale Caslavska *et al.* used an apparatus with a total processing volume of 130 ml, which used recycling ITP to isolate human serum transferrin, a metal-binding glycoprotein which has a concentration of about 2.5 mg/ml [14]. The transferrin concentration has a ratio of 1:17 when compared to human serum albumin, and the device was

determined to be adequate for preparative scale usage. However, separation of species with a higher dynamic range require smaller apparatuses, such as the 20 ml vortex stabilized electrophoresis apparatus at WSU, where preliminary experiments demonstrated separation of model proteins with a concentration ratio of 700:1.

The use of miniaturized analytical separation devices has many potential benefits over the use of conventional equipment, including improved analytical performance, reduced analysis times, low manufacturing costs, and reduction in reagent and sample consumption [15], while for preparative scale, larger instrumentation is required. Research on ITP has been done to explore instrumentation from milliliter to sub microliter capacities.

During the last decade, capillary electrophoresis has gained a lot of popularity, and is routinely used in laboratories [16]. Capillary isotachophoresis (CITP) benefited from the development of capillary zone electrophoresis (CZE), since both these methods can be done in the same instrumentation [4]. On-line CITP-CZE has been used for many applications, including pharmaceuticals, food, lipoproteins, and waste water analyses [5].

Gysler *et al.* compared the utility of CITP-CZE and high performance size-exclusion chromatography (HPSEC) for the determination of dimeric and monomeric recombinant human interleukin-6 [16]. Using fused silica capillaries, 75 μm I.D. X 360 μm O.D., cut to a total length of 70 cm, two physically different forms of dimeric interleukin-6 were revealed using

CITP-CZE. In comparison, HPSEC was not able to separate the two different forms, and required 20 times more protein for analysis [16].

Trace impurity analysis of synthetic and natural organic compounds using CITP coupled with nuclear magnetic resonance (NMR), was conducted in 2002, by Wolters *et al.* [17]. Their results showed that a 10^3 excess of sucrose (200 mM) over atenolol (200 μM) could be resolved using CITP-NMR, while concentrating the atenolol 200-fold. Research on the determination of trace iodide in sea water illustrated that CITP-CZE was successful for the direct determination of sub to low μg l^{-1} levels [18].

Previous work on ITP has shown that it is a suitable method for both meso and micro scales, and is applicable to the purification of species with a high dynamic range. The present work examines ITP zone behavior at the meso scale and micro scale, focusing on zone immobilization, and zone behavior following a 180° turn.

1.4 References

1. Human Proteomics Initiative. http://us.expasy.org/sprot/hpi/ (November 3, 2003),
2. Anderson, N. L., Anderson, N. G., The Human Plasma Proteome. *Molecular and Cellular Proteomics* **2002,** 1, (11), 845-867.
3. Everaerts, F. M., Becker, J. L., Verheggern, Th. P. E. M., *Isotachophoresis: Theory, Instrumentation and Applications*. Elsevier Scientific Publishing Company: Amsterdam, 1976; Vol. 6.
4. Gebauer, P., Caslavska, J., Thormann, W. J., Innovative developments in isotachophoresis (displacement electrophoresis). *J. Biochem. Biophys. Methods* **1991,** 23, 97-105.
5. Gebauer, P., Boček, P., Recent progress in capillary isotachophoresis. *Electrophoresis* **2002,** 23, 3858-3864.
6. Gebauer, P., Boček, P., Theory of zone separation in isotachophoresis: A diffusional approach. *Electrophoresis* **1995,** 16, 1999-2007.
7. Šlais, K., Model of isotachophoresis (displacement electrophoresis) in tapered capillaries. *Electrophoresis* **1995,** 16, 2060-2068.
8. Křivánková, L., Boček, P., Continuous free flow electrophoresis. *Electrophoresis* **1998,** 19, 1064-1074.
9. Canut, G., Bauer, J., Weber, G., Separation of plant membranes by electrophoretic migration techniques. *J. Chromatogr. B* **1999,** 722, 121-139.

10. Chartogne, A., Reeuwijk, B., Hofte, B., van der Heijden, R., et al., Capillary electrophoretic separations of proteins using carrier ampholytes. *J. Chromatogr. A* **2002,** 959, 289-298.

11. Wainright, A., Williams, S. J., Ciambrone, G., Xue, Q., et al., Sample pre-concentration by isotachophoresis in microfluidic devices. *J. Chromatogr. A* **2002**, (979), 69-80.

12. Mohan, D., Paša-Tolić, L., Masselon, C. D., Tolić, N. et al., Integration of electrokinetic-based multidimensional separation/concentration platform with electrospray ionization-fourier transform ion cyclotron resonance-mass spectrometry for proteome analysis of Shewanella oneidensis. *Anal. Chem.* **2003,** 75, 4432-4440.

13. Křivánková, L., Gebauer, P., Boček, P., Some practical aspects of utilizing the on-line combination of isotachophoresis and capillary zone electrophoresis. *J. Chromatogr. A* **1995,** 716, 35-48.

14. Caslavska, J., Thormann, W., Isolation of human serum transferring by free-fluid recycling electrophoresis in simple buffers. *Electrophoresis* **1994,** 15, 1176-1185.

15. Prest, J. E., Baldock, S. J., Fielden, P. R., Goddard, N. J., Treves Brown, B. J., Miniaturised isotachophoretic analysis of inorganic arsenic speciation using a planar polymer chip with integrated conductivity detection. *J. Chromatogr. A* **2003,** 990, 325-334.

16. Gysler, J., Mazereeuw, M., Helk, B., Heitzmann, M., et al., Utility of isotachophoresis-capillary zone electrophoresis, mass spectrometry and high performance size-exclusion chromatography for monitoring interleukin-6 dimer formation. *J. Chromatogr. A* **1999,** 841, 63-73.

17. Wolters, A. M., Jayawickrama, D. A., Larive, C. k., Sweedler, J. V., Capillary isotachophoresis/NMR: Extension to trace impurity analysis and improved intrumental coupling. *Anal. Chem.* **2002,** 74, 2306-2313.

18. Ito, K., Ichihara, T., Zhuo, H., Kumamoto, K., et al., Determination of trace iodide in seawater by capillary electrophoresis following transient isotachophoretic preconcentration comparison with ion chromatography. *Analytica Chimica Acta* **2003,** 497, 67-74.

CHAPTER TWO

PREDICTION OF THE LOCATION OF STATIONARY STEADY-STATE ZONE POSITIONS IN COUNTERFLOW ISOTACHOPHORESIS PERFORMED IN A VORTEX-STABILIZED ANNULAR COLUMN

Schurie L. M. Harrison, Cornelius F. Ivory

School of Chemical Engineering and Bioengineering

Washington State University

Abbreviations: EACA, epsilon-amino-n-caproic-acid; **HCl,** Hydrochloric Acid; **LE,** Leading Electrolyte; **TE,** Trailing Electrolyte

Keywords: Analytical Expression/ Immobilization/ Isotachophoresis/ Modeling

Abstract

A theoretical model is presented and an analytical expression derived to predict the locations of stationary steady-state zone positions in isotachophoresis (ITP) as a function of current for a straight channel under a constant applied voltage. Stationary zones may form in the presence of a countercurrent flow whose average velocity falls between that of a pure leader zone and of a pure trailer zone. A comparison of model predictions with experimental data from an anionic system shows that the model is able to predict the location of protein zones with reasonable accuracy once the ITP stack has formed. This result implies that an ITP stack can be precisely directed by the operator to specific positions in a channel whence portions of the stack can be removed or redirected for further processing or analysis.

2.1 Introduction

Isotachophoresis (ITP) is a suitable fractionation and concentration technique for a variety of different sample types including food additives [1], drugs in biological samples [2], and recombinant proteins [3], and it is well suited for multiple scales ranging from microchip [4] to preparative applications [5]. Currently there is a great deal of interest in using ITP in microchips due to their small sample size and rapid separation [4]. Electrophoretic separation techniques, including ITP, do not require high pressures, packings or miniature pumping devices, which makes them ideal for use on microchips [6].

ITP is an electrophoretic separation method which utilizes a discontinuous buffer system [7, 8] comprised of a leading and trailing electrolyte having the highest and lowest mobilities, respectively, of all constituents in a target sample. A complex analyte sample is placed between the leading and trailing electrolytes, and some time after current is applied, those analytes with the same charge sign as the leading ion will stack themselves into a "train" of contiguous self-sharpening zones based on their electrophoretic mobilities. In the absence of a hydrodynamic counterflow, the ITP train will reach a constant, pseudo steady-state velocity that is governed by the mobility of the leading analyte and the conductivity of the leading electrolyte.

At steady-state, the concentration within each analyte zone increases until it is proportional to the concentration of the leading electrolyte, which allows for simultaneous fractionation and concentration of dilute sample species. For this reason ITP is an attractive preconcentration step [9], which has been coupled online with capillary zone electrophoresis (CZE) for many

applications including monitoring protein formation [10], determining trace iodide in seawater [11], and determining drugs in serum [2]. The concentrating ability of ITP makes it a suitable candidate for use in processing low abundance species, which is one of the major problems facing proteomics research today [12].

There has been a significant amount of work done on computer modeling of ITP [13-16]. In 1983, Bier et al. developed a general, nonlinear model for all electrophoretic transport modes including zone electrophoresis, isoelectric focusing and ITP [17]. This model assumed a one dimensional, isothermal system and was comprised of a set of nonlinear partial differential and algebraic equations, requiring numerical methods for quadrature. This model was modified in subsequent papers to account for various parameters including the effects of ionic strength on protein mobility [18, 19], electroosmosis [20], and bulk flow [21].

The application of a bulk flow, countercurrent to isotachophoretic transport has been applied as early as 1966 by Preetz [22]. Counterflow applied at appropriate rates can immobilize the ITP train. Immobilization of the ITP train has been used for recycling ITP of ovalbumin and lysozyme [23] and for CZE-ITP coupling [24].

In 1995, Thormann et al. expanded the model developed in 1983 by Bier et al. to investigate the impact of electroosmosis on ITP in capillaries [25]. Electroosmotic flow was assumed to be plug flow and was calculated based on the specific wall mobility, voltage gradient, pK of the wall, and pH of the solution. Their model provides concentration, pH and conductivity profiles as a

function of time. Computer simulation of an anionic ITP system showed that, under an applied current and with a counterflow of appropriate magnitude, the net velocity of the zones slowed asymptotically to zero. This demonstrated that a balance between electroosmotic counterflow and isotachophoretic migration leads to the evolution of a stationary steady-state zone in capillary ITP. Experiments performed in fused silica capillaries confirmed the formation of a stationary steady-state zone in ITP [25].

In the present work it is shown that one can stop the ITP train at any chosen position within the channel. An algebraic model is derived which predicts the locations and breadth of these stationary steady-state zones in ITP. Unlike the models on counterflow ITP published to date, this model has an analytical solution which allows quick determination of zone position as a function of the current at a fixed voltage. To test the model predictions, ITP experiments were conducted in a preparative scale apparatus [26] from which data was obtained by measuring zone position and current for a series of counterflow velocities. As counterflow velocity is increased, the current increases proportionately, and the stationary position of zones moves closer to the cathode or anode for an anionic or cationic system, respectively. A comparison of theory with experiment shows that the model was consistently able to predict zone position within the 95% confidence interval of the data. The average difference between experimental and predicted zone positions was 18%.

2.2 Materials and Methods

2.2.1 Chemicals

Bovine serum albumin (BSA), bovine hemoglobin (Hb) and 6-aminohexanoic acid (EACA) were obtained from Sigma (St. Louis, MO). Trizma base was purchased from Invitrogen (Carlsbad, CA), hydrochloric acid from Fisher Scientific (Hampton, NH), and bromophenol blue from Bio-Rad (Hercules, CA). Nanopure water came from a Barnstead Thermolyne (Dubuque, IA) Nanopure® Infinity UV/UF system.

2.2.2 Electrolyte and Sample Preparation

The leading electrolyte (LE) was 0.01 M hydrochloric acid adjusted to pH 9.5, and the trailing electrolyte (TE) was 0.06 M EACA adjusted to pH 10. The pH of the LE and TE were adjusted using Trizma base, which also served as the counterion. So that the BSA band was visible, bromophenol blue, which binds to BSA, was added to the LE in a 1:1 molar ratio to make a 10 mg/ml "blue albumin" solution. Bovine hemoglobin was dissolved in LE to make a 10 mg/ml Hb solution.

2.2.3 Instrument

ITP experiments were performed in a vortex-stabilized electrophoresis apparatus designed by Ivory and Gobie [27] which has recently been described in detail [26]. Briefly, the apparatus has a complementary grooved boron nitride rotor inside a Plexiglas® stator, which together forms an annulus in which the separation takes place. Spinning the rotor at 50 RPM creates stable vortices in the annulus that are similar in structure to, but distinctly different from, Taylor vortices. The

vortices prevent axial mixing of the fluid due to natural convection and provide improved heat and mass transfer via radial circulation of the vortices.

Cooling was provided to the apparatus by circulating a Syltherm XLT coolant oil (Dow, Midland, MI) at 10 °C through the inside of the hollow rotor using a MGW Lauda RC3 circulator (Brinkman, Westbury, NY). A Spellman SL300 power supply (Hauppauge, NY) provided the power to the electrodes and counterflow was applied using a Buchler Instruments multistatic® pump (Lenexa, KS).

2.2.4 ITP Procedure

In each experiment, the anode was located at the bottom of the column and the cathode at the top with LE and TE used as analyte and catholyte, respectively. Figure 2.1 shows a picture of the apparatus with relevant parts marked. Due to the high pH of the system, all of the ions being separated were anions; therefore the electrophoretic movement of the sample ions was toward the anode located at the bottom of the column.

Before each run, the bottom half of the column was filled with LE using a syringe mounted on a port at the anodic end of the column. The top half of the annulus was filled with TE using a syringe mounted at the center of the column. Then, a protein sample containing 30 mg BSA and 30 mg Hb at a concentration of 10 mg/ml in LE was injected between the two electrolytes. After the sample was injected, a constant electric field was applied across the column and a counterflow was applied to the annulus by pumping LE into the bottom of the column.

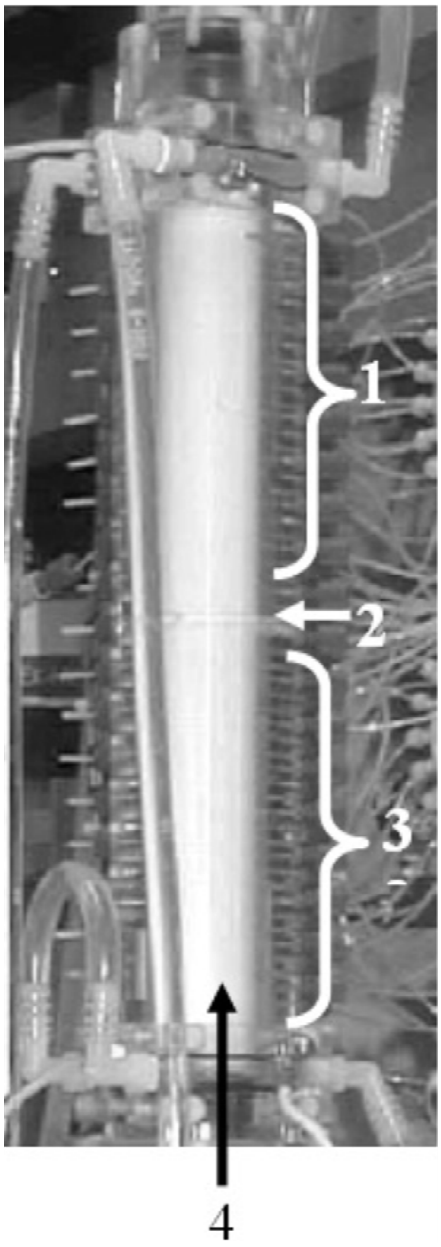

Figure 2.1: Photograph of the vortex-stabilized electrophoresis apparatus used for ITP. At the beginning of each ITP experiment the annulus was filled with trailing electrolyte (1) and leading electrolyte (3). Sample was then injected between the electrolytes (2). Counterflow (4) was applied at the anodic end of the apparatus, countercurrent to isotachophoretic migration.

2.2.5 Theory

Our model assumes that the system is at steady-state, which means that the train is fully formed and that it has reached its final, stationary position. It includes only the sample species being separated, the leading and trailing ions, and a single counterion. It is assumed that each zone is pure, meaning that a zone contains only one coion and one counterion. Overlap between bands due to dispersion, as well as salt effects and double layer effects are neglected.

A unique characteristic of ITP is that all species move at the same speed once steady-state has been reached. The velocity of each species moving in an electric field is calculated by multiplying its electrophoretic mobility by the electric field strength; therefore in ITP,

$$\mu_{LE} E_{LE} = \mu_j E_j = \mu_{TE} E_{TE}, \qquad (1)$$

where μ_j is the electrophoretic mobility of the j^{th} component and E_j is the electric field strength in the j^{th} zone. The subscripts LE, TE, and j represent the leading electrolyte, trailing electrolyte and each of the sample species in their respective zones. The electrophoretic mobility of a species is dependent on many factors including temperature, ionic strength, and pH but, in this derivation, they are assumed to be constant within each zone.

It is further assumed that a single counterion, represented by subscript m, is present in varying concentrations in each zone in order to ensure electroneutrality within that zone. Equations 2a through 2c represent electroneutrality for a leading electrolyte zone, a single sample zone, and a trailing electrolyte zone, respectively

$$z_{LE}c_{LE} + z_m c_{mLE} = 0 \tag{2a}$$

$$z_j c_j + z_m c_{mj} = 0 \tag{2b}$$

$$z_{TE}c_{TE} + z_m c_{mTE} = 0\,, \tag{2c}$$

where z represents charge valence and c represents concentration. Since the concentration of the counterion varies within each zone, a second subscript is used to specify the zone that is being considered, for example c_{mLE} is the concentration of the counterion, m, in the leading zone.

The current in the j^{th} zone can be described by the equation

$$i_j = \sigma_j E_j A, \tag{3}$$

where i_j is the current, σ_j is conductivity, E_j is electric field strength, and A is the cross sectional area of the separation chamber, which is assumed constant along the channel. By expanding the conductivity in terms of the ionic concentrations, we can write for the current in each zone

$$i_{LE} = F(z_{LE}\mu_{LE}c_{LE} + z_m\mu_m c_{mLE})E_{LE}A \tag{4a}$$

$$i_j = F(z_j\mu_j c_j + z_m\mu_m c_{mj})E_j A \tag{4b}$$

$$i_{TE} = F(z_{TE}\mu_{TE}c_{TE} + z_m\mu_m c_{mTE})E_{TE}A\,, \tag{4c}$$

where F is Faraday's constant. The current in each discrete zone is the same, thus

$$i_{LE} = i_j = i_{TE}\,. \tag{5}$$

The following equations for the total voltage drop across the column and total length of the column, respectively, for a system of n components in our sample are:

$$V_T = E_{LE} L_{LE} + \sum_{j=0}^{n} E_j L_j + E_{TE} L_{TE} \tag{6}$$

$$L_T = L_{LE} + \sum_{j=0}^{n} L_j + L_{TE}, \tag{7}$$

where L is the length of a zone and the subscript, T, represents total.

The concentration of each component in its respective zone is

$$c_j = \frac{M_j}{L_j A}, \tag{8}$$

where M_j is the mass of species j in that zone.

In fully-developed ITP, the plateau concentration in each zone is dependent on the concentration of the leading electrolyte. By solving Eqs. 1-5, one obtains the following relationships for the plateau concentration of the trailing electrolyte and sample species [28]

$$\frac{c_{TE}}{c_{LE}} = \frac{z_{LE}(\mu_{LE} - \mu_m)\mu_{TE}}{z_{TE}(\mu_{TE} - \mu_m)\mu_{LE}} \tag{9a}$$

$$\frac{c_j}{c_{LE}} = \frac{z_{LE}(\mu_{LE} - \mu_m)\mu_j}{z_j(\mu_j - \mu_m)\mu_{LE}}. \tag{9b}$$

From this solution it is seen that the plateau concentration of each zone is dependent only on the properties of the leading electrolyte, the particular zone species and the counterion, and is independent of the other species present in the system. This shows that the plateau concentration of a sample zone does not depend on the amount of sample present or on the electric field. From the relationship given in Eq. 8 one can see that the length of the sample zone increases

proportionally with increasing mass. Therefore, once a species achieves its plateau concentration, zone length can be used as a direct measure of its total mass.

By solving Eqs. 1, 2, and 4-8 simultaneously, algebraic expressions are obtained for the length of each zone, which allows prediction of the position of each band interface in the sample train. Here, the position of the train is defined as the interface between the leading electrolyte and the first sample zone relative to the front edge of the separation chamber. To predict this position, Eqs. 1-8 were solved to obtain the length of the leading zone as a function of the current

$$L_{LE} = -\frac{i_{LE}\mu_{LE}^{\,2}\left[\sum_{j=0}^{n}\frac{\alpha_j}{\gamma} + L_T\left(\frac{\mu_m}{\mu_{LE}} - 1\right)\right] + FV_T\mu_{TE}\gamma(\mu_{LE} - \mu_m)^2}{i_{LE}(\mu_{LE} - \mu_m)(\mu_{LE} - \mu_{TE})} \tag{10a}$$

where

$$\alpha_j = M_j z_j \left(1 - \frac{\mu_{TE}}{\mu_j}\right)\left(1 - \frac{\mu_m}{\mu_j}\right) \tag{10b}$$

and

$$\gamma = z_{LE} c_{LE} A\,. \tag{10c}$$

The length of the sample zones can be calculated from the following:

$$L_j = \frac{M_j z_j \mu_{LE}(\mu_j - \mu_m)}{\gamma\mu_j(\mu_{LE} - \mu_m)}\,. \tag{11}$$

The current can be adjusted by varying the counterflow rate applied to the system. At steady-state the counterflow velocity will be equal to and opposite to the velocity of the zones. Substitution of the counterflow velocity, v_{CF}, into Eq. 4a and simplification using the electroneutrality condition (Eq. 2a), yields a direct relationship between current and counterflow velocity:

$$i_{LE} = v_{CF} F \gamma \left(\frac{\mu_m}{\mu_{LE}} - 1 \right). \tag{12}$$

Upper and lower limits of the counterflow rate appropriate for stopping the zones within a separation chamber can be estimated by substituting Eq. 12 for the current in Eq. 10a for a system with no sample species, and solving for the counterflow velocity:

$$v_{CF} = \frac{V_T \mu_{TE} \mu_{LE}}{L_{LE}(\mu_{LE} - \mu_{TE}) - L_T \mu_{LE}}. \tag{13}$$

The length of the leading electrolyte zone in Eq. 13 can then be set to zero and to the total length of the separation chamber to approximate a suitable range of counterflow velocities.

In order to make quantitative predictions using this model, the electrophoretic mobilities and charges of all species, the masses of all sample species, and the concentration of the leading electrolyte must be specified. The cross sectional area and length of the separation chamber and the voltage across the separation chamber are also required.

2.3 Results and Discussion

ITP was performed in a vortex-stabilized electrophoresis apparatus as described above. For each experiment, the voltage was set at a constant value of 2.50 kV and the current was allowed to adjust to its steady-state value depending on the conditions set. A set of counterflow rates ranging from about 0.002 to 0.02 cm/s were used to control the current. As the counterflow velocity is increased, the steady-state position of the sample train is shifted towards the cathode, and the LE fills more of the annulus. Since the LE has a higher conductivity than the other species in the column, the current will increase as the counterflow velocity is increased, according to Eq. 12. The minimum and maximum counterflow rates were chosen such that no part of the sample train would migrate beyond the anode or cathode.

The system was allowed up to 12 hours to reach steady-state at each counterflow rate. When the sample was first introduced, and the voltage applied, distinct protein bands with sharp front and rear boundaries formed within 30 minutes. The sample train then began moving toward its steady-state position and arrived there approximately 5 hours after the start of the experiment. By moving to smaller scales, such as a microchip, separation times can be greatly reduced.

Figure 2.2 shows a photograph of the contiguous protein zones at two steady-state positions. At an experimental pH of 9.5, blue albumin has a greater electrophoretic mobility than hemoglobin and therefore forms the front protein zone. The figure of the sample train at 9.6 mA shows a clear band between the blue albumin and hemoglobin bands which is most likely “free” BSA, that is BSA which does not have bromophenol blue bound to it. As the current was increased,

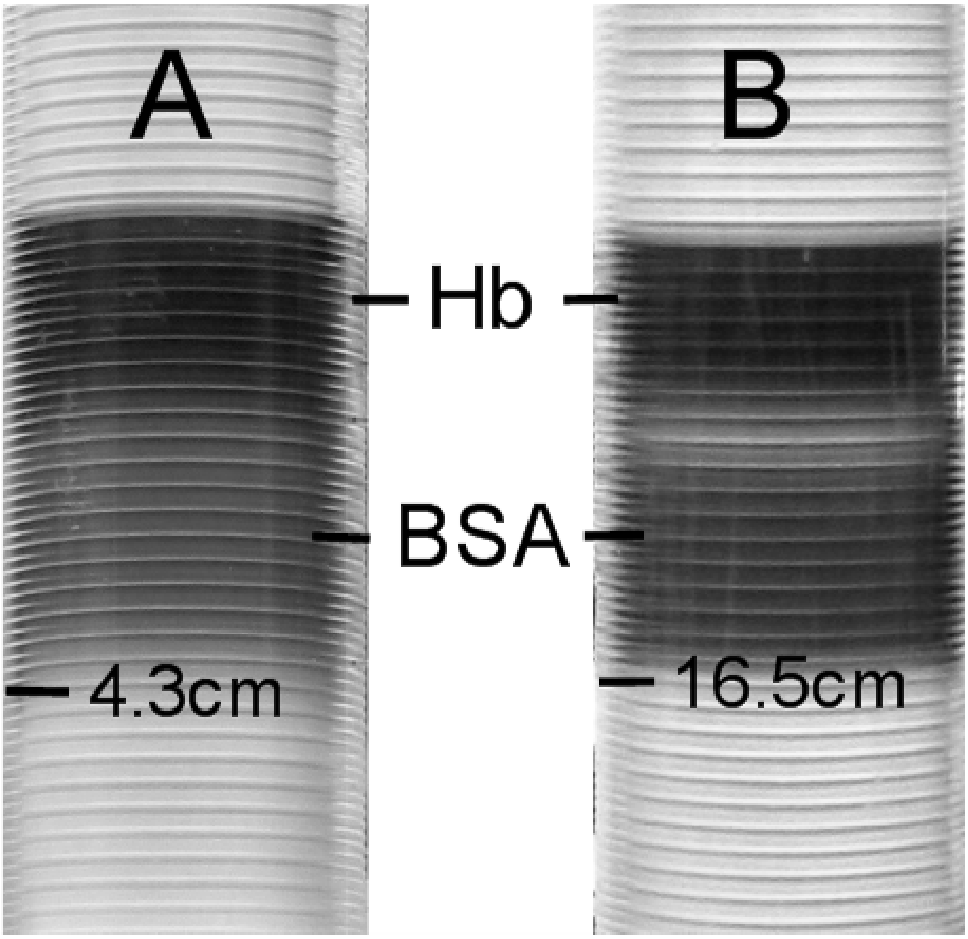

Figure 2.2: Photograph showing the isotachophoretic separation of 30 mg BSA and 30 mg Hb at a voltage of 2.50 kV and a current of A) 4.3 mA and B) 9.6 mA.

the edges of both sample zones became sharper, which is seen in Figure 2.2. However, as the sample train neared the cathode, there was some dispersion of the Hb zone. This dispersion is likely due to the fact that the fluid flow near the cathode is disturbed by the presence of an opening for the electrode housing. No data was collected above a current of 24.1 mA because the Hb zone began exiting the system at this point.

Modeling was performed by solving the set of non-linear algebraic equations (Eqs. 1-8), which describe steady-state ITP. An analytical solution was obtained for the length of the leading electrolyte zone as a function of the current. By choosing to model the length of the leading electrolyte zone, the position of the beginning of the sample train is obtained. If desired, one could also solve for the length of each individual zone (Eq. 11) to predict the position of each zone interface.

A system consisting of only a leading and a trailing electrolyte was initially modeled, using Eq. 10, to illustrate the response of zone position to current. From this solution it is shown that, as the current is increased via increasing the counterflow velocity, the fraction of the annulus that is filled with LE increases asymptotically. With the addition of 30 mgs of two sample proteins, the resulting curve has the same shape as that of a system with no sample, but is shifted down. Figure 2.3 shows the length of the leading zone for both a system with only a leading and trailing zone and for the same system with two sample species added. Figure 2.3 is based on a system with an annulus length of 29 cm, a cross-sectional area of 0.685 cm^2 and a constant voltage of 2.50 kV. The relevant properties of all species in the system are shown in Table 2.1.

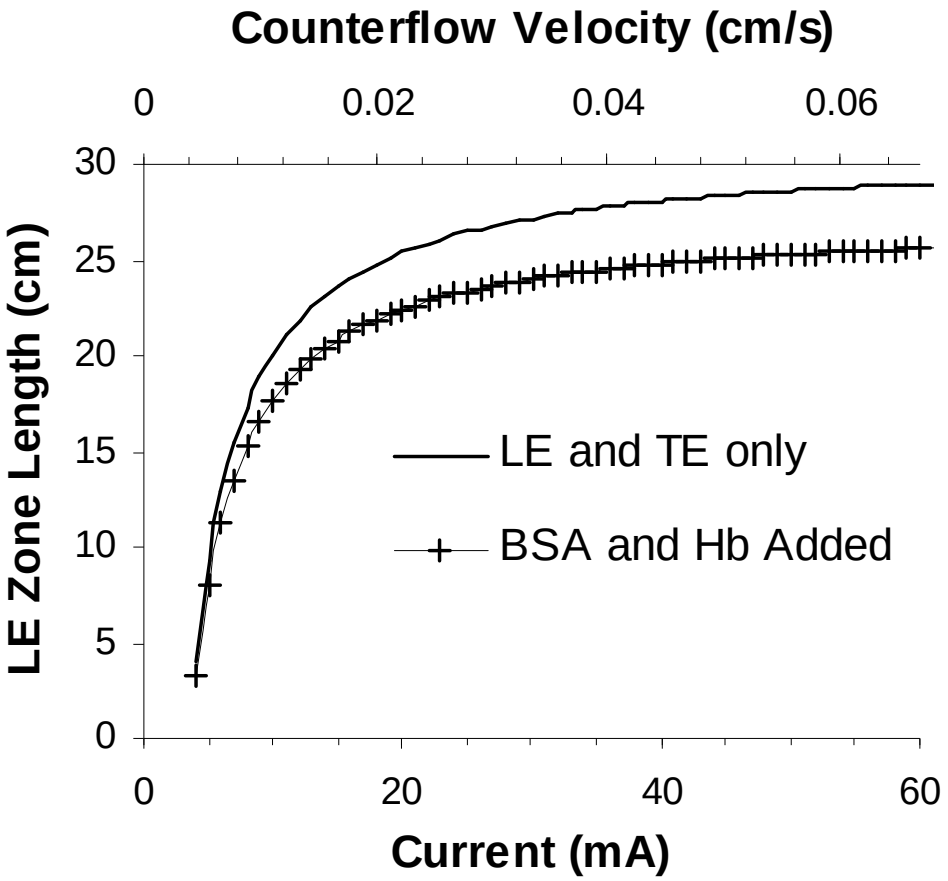

Figure 2.3: Model predictions of the length of the leading electrolyte zone as a function of current comparing a system containing only a leading and trailing electrolyte to a system with 30 mg BSA and 30 mg Hb added. Predictions are made for a system with a constant applied voltage of 2.50 kV. The leading electrolyte is 0.01 M HCl, pH 9.5, and the trailing electrolyte is 0.06 M EACA, pH 10.0.

Table 2.1: Parameters used for Model Calculations

Zone	Species	Charge	Mobility[a]
Leading	Cl-	-1	-7.91 [7]
Trailing	EACA	-0.14[b] [30]	-0.40[c] [31]
Sample 1	BSA	-25 [32]	-3.25 [33]
Sample 2	Hb	-12 [34]	-1.20[c] [35]
Counterion	Tris	0.96[b] [30]	2.84[c] [31]

a) Net electrophoretic mobility in units of $m^2V^{-1}s^{-1}\times10^8$.

b) Calculated based on pK values from cited reference.

c) Calculated by multiplying the absolute mobility from the cited reference by the charge.

Data sets were collected for three experiments, (E1-E3), with a BSA/Hb sample as described above. Model predictions are compared to the experimental data in Figure 2.4 which shows that the model accurately predicts that, as the current increases due to an increase in counterflow velocity, the length of the leading zone increases asymptotically. A statistical analysis of the data was conducted using the Matlab 7.0 curve fitting tool to calculate a 95% prediction interval [29] for the future response of experimental data. This interval includes the error in estimating the mean and the variation in the data to predict that 95% of future data collected for zone position as a function of current will fall between the upper and lower limits. Although the predicted LE zone length comes near the upper limit of the 95% prediction interval for currents between 5-7 mA, all points in the model are within the 95% prediction interval, which shows that it is able to predict the position of the steady-state stationary zone to within experimental variation.

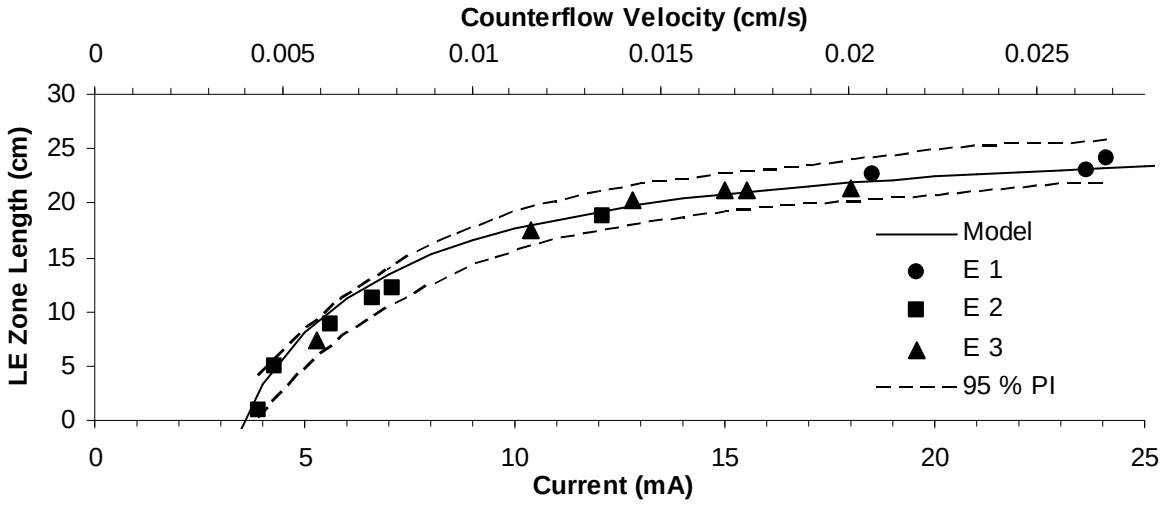

Figure 2.4: Comparison of model predictions to experimental data for the length of the leading electrolyte zone. The experiment was conducted three times in order to obtain data sets, represented by E 1 through E 3. The dashed line shows the 95% prediction interval (PI) for the experimental results, based on data analysis. Model input parameters were identical to the experimental conditions when possible. Literature values of properties were used for parameters not directly measured during the experiment, shown in Table 2.1.

2.4 Concluding Remarks

The model presented in this paper produces an analytical solution which can be used to accurately predict the positions of the stationary steady-state zones formed during ITP. By varying the countercurrent velocity, within the calculated bounds, the ITP train can be immobilized at any position within the channel. We have shown that these positions can be predicted as a function of the current, given a constant voltage, which gives us the ability to stop the train at any point in a channel.

From these results, it appears that the assumptions made in the development of our model are valid for this apparatus under our experimental conditions. One assumption is that dispersion is negligible. In free-flow electrophoresis, conductivity gradient instability has been reported, which causes significant dispersion [36]. In unpublished free-flow ITP experiments performed in our lab in a channel without vortex stabilization, conductivity gradient instability was observed above a certain voltage, which caused significant dispersion of the ITP train between the Hb and TE zones. The agreement between the model and our experimental results in the present work show that the vortex stabilized electrophoresis apparatus stabilized the fluid and decreased dispersion. Experimental results showed that dispersion was more pronounced at low currents but, even in this region, the model is able to predict the behavior of the stationary steady-state zone with reasonable accuracy.

Temperature effects were not considered in this model. Since Joule heating is the product of the electric field strength with the current and since we are working with a constant current, then the

temperature of zones will increase as electrophoretic mobility decreases [28]. Therefore there will be temperature variation during separation. Species parameters, such as pK and electrophoretic mobility are dependent on temperature as well as other variables including ionic strength. Neither temperature nor ionic strength were measured directly or predicted for this experiment. Values used as input parameters were those found in literature for a temperature of either 20 °C or 25 °C and an ionic strength ranging from zero to 0.01 M. Our results show that our model was able to predict stationary steady-state zone positions in agreement with experimental data, despite neglecting temperature variation.

2.5 Acknowledgements

This material is based upon work supported in part by the National Institute of General Medical Sciences/National Institutes of Health (Grant # GM008336) and the Chemical Engineering Department at Washington State University.

2.6 References

[1] Bodor, R., Žúborová, M., Ölvecká, E., Madajová, V., et al., *J. Sep. Sci.* 2001, *24*, 802-809.

[2] Ölvecká, E., Koníková, M., Grobuschek, N., Kaniansky, D., Stanislawski, B. J., *J. Sep. Sci.* 2003, *26*, 693-700.

[3] Stowers, A. W., Spring, K. J., Saul, A., *Bio/Technology* 1995, *13*, 1498-1503.

[4] Jeong, Y., Choi, K., Kang, M. K., Chun, K., Chung, D. S., *Sensors and Actuators B* 2005, *104*, 269-275.

[5] Hoffstetter-Kuhn, S., Kuhn, R.; Wagner, H., *Electrophoresis* 1990, *11*, 304-309.

[6] Walker, P. A. I., Morris, M. D., Burns, M. A., Johnson, B. N., *Anal. Chem.* 1998, *70*, 3766-3769.

[7] Thormann, W., Mosher, R. A., *Electrophoresis* 1990, *11*, 292-298.

[8] Gebauer, P., Caslavska, J., Thormann, W. J., *J. Biochem. Biophys. Methods* 1991, *23*, 97-105.

[9] Gebauer, P., Boček, P., *Electrophoresis* 2002, *23*, 3858-3864.

[10] Gysler, J., Mazereeuw, M., Helk, B., Heitzmann, M., et al., *J. Chromatogr. A* 1999, *841*, 63-73.

[11] Ito, K., Ichihara, T., Zhuo, H., Kumamoto, K., et al., *Analytica Chimica Acta* 2003, *497*, 67-74.

[12] Domon, B., Broder, S. J., *J. Proteome Res.* 2004, *3*, 253-260.

[13] Gebauer, P., Boček, P., *Electrophoresis* 1995, *16*, 1999-2007.

[14] Šlais, K., *Electrophoresis* 1995, *16*, 2060-2068.

[15] Šlais, K., *J. Chromatogr. A* 1997, *764*, 309-321.

[16] Baygents, J. C., Schwarz, B. C. E., Deshmukh, R. R., Bier, M. J., *J. Chromatogr. A* 1997, *779*, 165-183.

[17] Bier, M., Palusinski, O. A., Mosher, R. A., Saville, D. A., *Science* 1983, *219*, 1281-1287.

[18] Mosher, R. A., Dewey, D., Thormann, W., Saville, D. A., Bier, M., *Anal. Chem.* 1989, *61*, 362-366.

[19] Mosher, R. A., Gebauer, P., Caslavska, J., Thormann, W., *Anal. Chem.* 1992, *64*, 2991-2997.

[20] Mosher, R. A., Zhang, C. X., Caslavska, J., Thormann, W. J., *J. Chromatogr. A* 1995, *716*, 17-26.

[21] Deshmukh, R. R., Bier, M., *Electrophoresis* 1993, *14*, 205-213.

[22] Preetz, W., *Talanta* 1966, *13*, 1649-1660.

[23] Caslavska, J., Gebauer, P., Thormann, W., *J. Chromatogr.* 1991, *585*, 145-152.

[24] Reinhoud, N. J., Tjaden, U. R., van der Greef, J., *J. Chromatogr. A* 1993, *653*, 303-312.

[25] Thormann, W., Caslavska, J., Mosher, R. A., *Electrophoresis* 1995, *16*, 2016-2026.

[26] Ivory, C. F., *Electrophoresis* 2004, *25*, 360-374.

[27] Ivory, C. F., Gobie, W. A., United States 1994.

[28] Everaerts, F. M., Becker, J. L., Verheggern, Th. P. E. M., *Isotachophoresis: theory, instrumentation and applications*, Elsevier Scientific Publishing Company, Amsterdam 1976.

[29] Montgomery, D. C., Runger, G. C., Hubele, N. F., *Engineering Statistics*, John Wiley and Sons, New York 1998, p. 313.

[30] Lide, D. R. (Ed.), *CRC Handbook of Chemistry and Physics*, CRC Press, New York 1995, pp. 7-30, 38-50.

[31] Pospíchal, J., Gebauer, P., Boček, P., *Chem. Rev.* 1989, *1989*, 419-430.

[32] Tanford, C., Swanson, S. A., Shore, W. S. J., *J. Am. Chem. Soc.* 1955, *77*, 6414-6421.

[33] Caflisch, G. B. N., T.; Yu, H. J., *J. Colloid Interface Sci.* 1980, *76*, 174-181.

[34] De Bruin, S. H., Janssen, L. H. M., Van Os, G. A. J., *J. Biochim. Biophys. Acta* 1969, *188*, 207-215.

[35] Douglas, N. G., Humffray, A. A., Pratt, H. R. C., Stevens, G. W., *Chem. Eng. Sci.* 1995, *50*, 743-754.

[36] Lin, H., Storey, B. D., Oddy, M. H., Chuan-Hua, C., Santiago, J. G., *Phys. Fluids* 2004, *16*, 1922-1935.

CHAPTER THREE

ISOTACHOPHORESIS IN AN S CHANNEL: EXPERIMENT AND 2-D SIMULATION

Schurie L. M. Harrison, Cornelius F. Ivory

School of Chemical Engineering and Bioengineering

Washington State University

Abbreviations: CGI, conductivity gradient instability; **EACA**, epsilon-amino-n-caproic-acid; **HCl,** hydrochloric acid; **LE,** leading electrolyte; **PSSSD**, pseudo steady-state standard deviation; **TE,** trailing electrolyte

Keywords: Isotachophoresis/ Recovery Distance/ S Channel/ Simulation

Abstract

ITP in a two turn S channel was simulated using Comsol Multiphysics v 3.3 and conducted experimentally in a free-flow apparatus developed by the authors. Our simulation results show that ITP zones are able to return to an isotachophoretic *pseudo* steady-state given a sufficient length of straight channel following a turn. This recovery distance was found to be independent of voltage. Additionally, the recovery distance increased as total sample increased, and decreased as the turn radius increased. Experimental results showed that ITP was affected by a conductivity gradient instability at higher voltages, and increased dispersion at lower voltages. Our experimental results also showed that for our channel geometry and sample mass, dispersion due to the 180° turn was negligible.

3.1 Introduction

Isotachophoresis (ITP) is a self-sharpening electrophoretic technique that has the ability to both purify and concentrate analytes. For this reason ITP has been used for both purification and pre-concentration, often coupled to capillary zone electrophoresis [1-4]. In ITP, an analyte sample is placed between a leading electrolyte (LE) and a trailing electrolyte (TE), such that all of the constituents of the analyte sample have electrophoretic mobilities less than the LE and greater than the TE. Once an electric field is applied, all species with the same charge sign as the leading ion align into a "train" of adjoining zones according to their mobilities. A *pseudo* steady-state is attained when all zones in the ITP train move with constant, equal velocities. With an appropriate counterflow, a stationary steady-state can be achieved where the train comes to and remains at a fixed position within the separation channel [5, 6].

During the ITP process, the concentrations of analyte zones adjust so that they are proportional to the concentration of the leading electrolyte, allowing dilute sample analytes to be concentrated. Using a microchip, ITP has been shown to increase sample concentration by a millionfold in a single step assay [3]. There is a growing need for analysis of real samples, such as human blood, which include analytes in very low concentrations relative to other species, requiring techniques such as ITP that are able to both concentrate and purify these low abundance analytes [7]. Eventually, we would like a portable tool, likely in the form of a microchip, to analyze these complex samples [7]. Microchips have many advantages over larger scale separation devices, including the fact that separation of analytes

often takes only minutes or seconds, in partial due to small initial sample size and high electric fields [8].

In order to fit more separation length on a chip, turns in a channel are employed. Griffiths and Nilson have presented various geometries using turns connected with straight segments to increase the channel length on a chip [9]. Although turns increase the channel length, they also present a potential source of dispersion due to the difference in length and field strength across the channel width [10]. Several authors have studied ways to minimize dispersion due to turns when zone electrophoresis is employed, including reducing channel width in the turn [11], using a tapered geometry into a reduced turn width [12], and determining a minimum turn radius [9].

In this paper, the effects of turns in a channel on ITP are examined. Using a two turn S channel, 2-D modeling was performed using Comsol Multiphysics v 3.3. Results showed that the ITP train was able to "recover" some distance after a turn. The effects of voltage, turn radius, and sample quantity on the recovery distance are reported. The behavior of ITP zones around 180° turns was also observed experimentally in a two turn S channel developed by the authors.

3.2 Materials and Methods

3.2.1 Equipment

ITP was performed in an S apparatus developed by the authors. The separation channel had a constant width of 700 μm and constant height of 1 mm. The length of the channel between the electrodes was 19 cm. The channel has two 180° turns each with a turn radius 3.1 mm. The overall footprint of the apparatus used was 6 cm x 12 cm x 2 cm.

The channel was cut into a 0.3 cm alumina ceramic plate (Superior Technical Ceramics Corp., St. Albans, VT) and has a flat 1.2 cm thick plexiglass top, which allows the channel to be viewed from the top of the apparatus (Figure 3.1). The ceramic plate also has good heat transfer properties (thermal conductivity: 31 W/mK) to reduce the effects of Joule heating. A PDMS gasket was sandwiched between the ceramic plate and plexiglass in order to seal the channel. The ceramic plate, PDMS gasket, and plexiglass are held together by a set of eight bolts that surround the channel. A steel plate on top of the plexiglass is used to prevent the bolts from deforming the plexiglass when they are tightened.

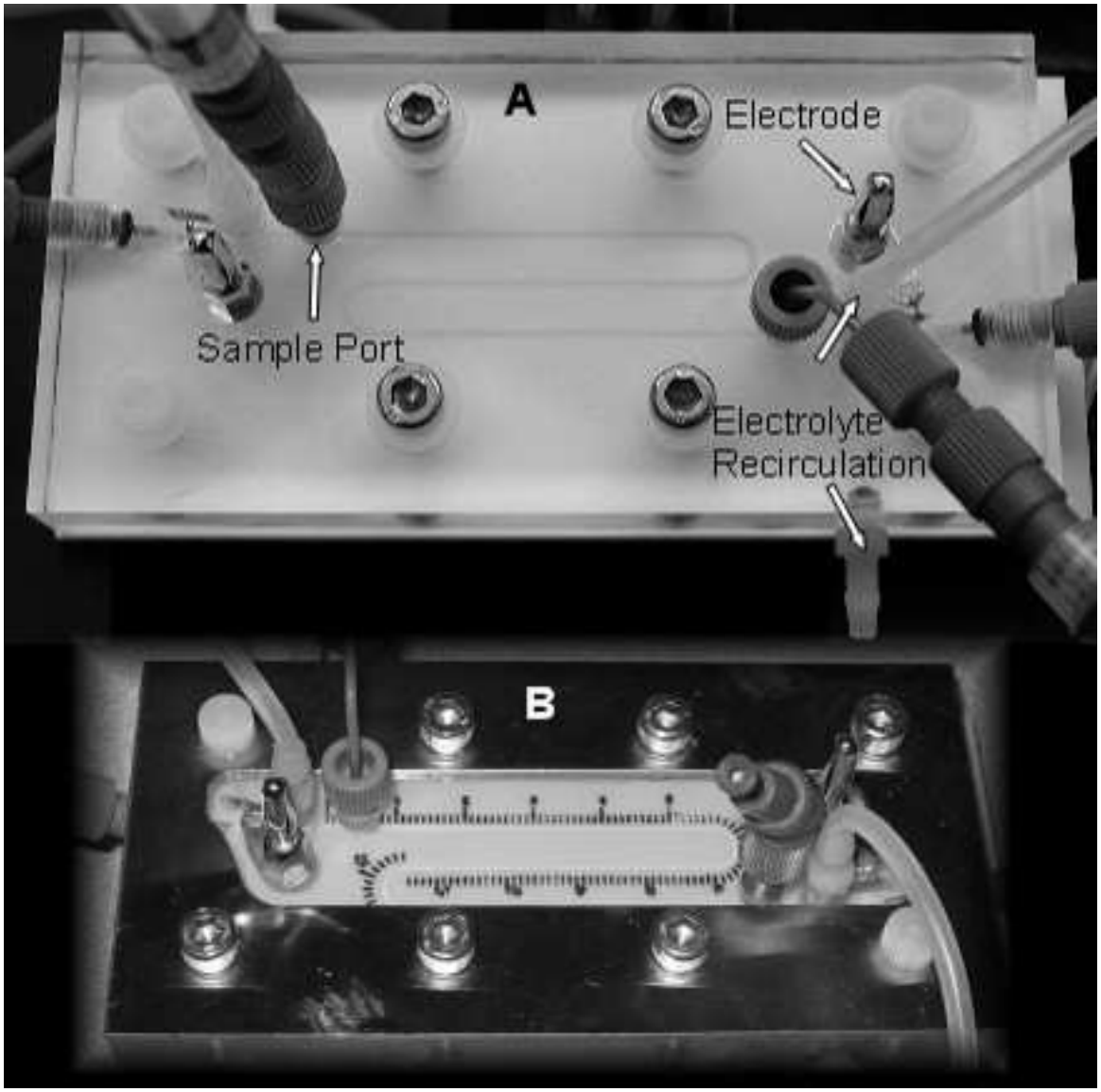

Figure 3.1: A) Photograph of S channel developed by the authors. Separation channel is 700 μm wide x 1 mm deep x 19 cm long. B) Photograph of the same apparatus with added steel plate and position scale.

The electrode reservoirs are cylinders cut into the plexiglass top, and separated from the channel by a 6000 MWCO dialysis membrane. An inlet and outlet into each electrolyte reservoir allows the electrolytes to be recirculated using a peristaltic pump (Buchler Instruments, Lenexa, KS). In order to reduce pulsing from the peristaltic pump, windkessels (translated: air chambers) were fashioned using a T-junction between the pump and the electrolyte recirculation inlet of the apparatus (Figure 3.2).

3.2.2 Chemicals and reagents

Bovine serum albumin (BSA), bovine hemoglobin (Hb) 6-aminohexanoic acid (EACA), and methylcellulose were obtained from Sigma (St. Louis, MO). Trizma base was purchased from Invitrogen (Carlsbad, CA), hydrochloric acid from Fisher Scientific (Hampton, NH), and bromophenol blue from Bio-Rad (Hercules, CA). Nanopure water came from a Barnstead Thermolyne (Dubuque, IA) Nanopure® Infinity UV/UF system.

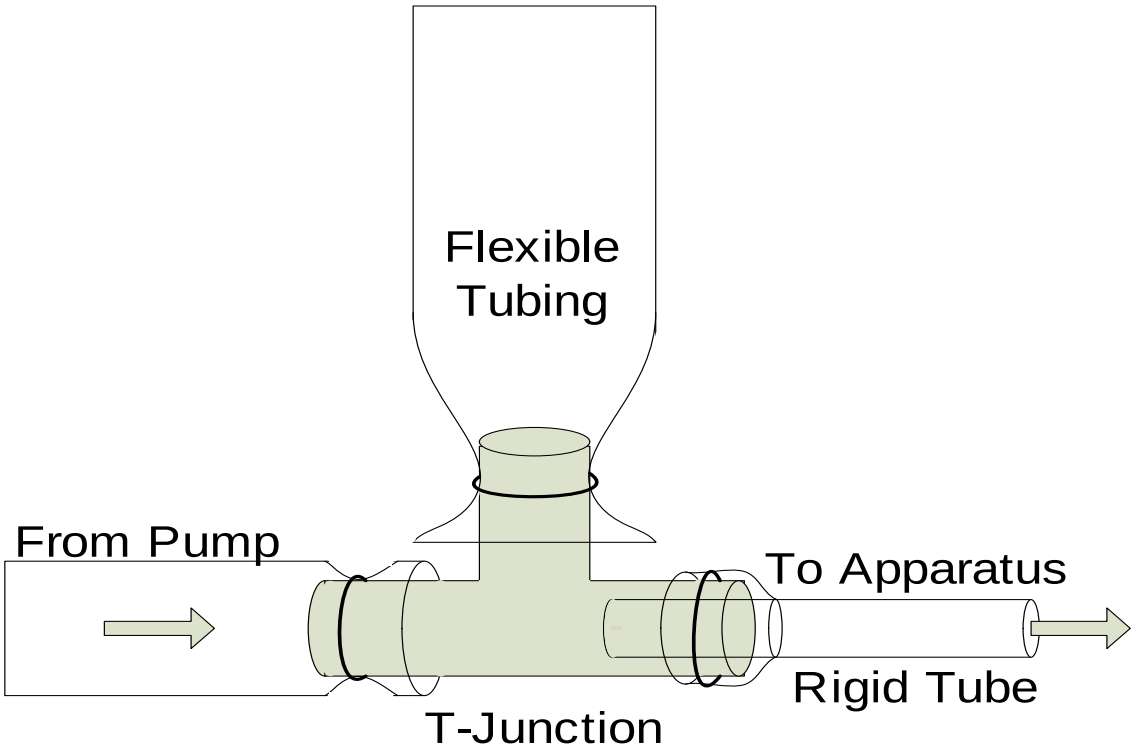

Figure 3.2: Design of a windkessel. Windkessels were placed between the peristaltic pump and the electrode reservoirs to reduce pulsing due to electrolyte circulation.

3.2.3 Electrolyte and Sample Preparation

The leading electrolyte (LE) was 0.01 M hydrochloric acid adjusted to pH 9.5, and the trailing electrolyte (TE) was 0.06 M EACA adjusted to pH 10. Trizma base, which served as the counterion, was used to adjust the pH of the LE and TE. A 10 mg/ml "blue albumin" solution was made by mixing bromophenol blue with BSA in a 1:1 molar ratio in LE. Bovine hemoglobin was dissolved in LE to make a 10 mg/ml Hb solution. A 0.4% methyl cellulose solution was prepared by combining with nanopure water.

3.2.4 Experimental procedure

To suppress electroosmostic flow in the channel, a 0.4% methyl cellulose solution was injected into the channel and allowed to set at least five minutes prior to the ITP run. The methyl cellulose was then removed, and the channel was filled with LE through a syringe at the anodic end of the channel. Using a 20 μl sample loop, protein sample at a concentration of 10 mg/ml was injected via the sample inlet located nearest the cathode. A valve at the cathodic end of the channel was closed during sample injection so that the sample was contained in the channel. LE was circulated through the electrolyte reservoir at the anode, and TE was circulated through at the cathode via a peristaltic pump. A fixed voltage was applied to the channel.

3.2.5 Theory

A two dimensional, transient ITP model is presented which assumes that there is no bulk flow or temperature gradients in the system. In a solution with an applied electric field all charged species can move by convection, electromigration, and diffusion. The flux of each species can be described by the Nernst-Planck equation,

$$J_i = C_i u - F z_i \mu_i C_i \nabla \Phi - D_i \nabla C_i \,, \tag{1}$$

where J_i is the flux of species i, C_i is the concentration of species i, u is the bulk flow velocity, F is Faraday's constant, z_i is the charge of species i, μ_i is the absolute mobility of species i, and Φ is the electric potential. In the present work, there is no bulk flow and thus the convection term, $C_i u$, equals zero.

The conservation of mass of each species is given by

$$\frac{\partial C_i}{\partial t} + \nabla \cdot J_i = R_i \,, \tag{2}$$

where t is time, and R_i is the rate of generation of species i. Our model assumes no generation for all species; hence R_i is zero for all species.

Electroneutrality is conserved over the entire channel, and is given by

$$\Sigma z_i C_i = 0 \,. \tag{3}$$

Thus current conservation can be described by

$$\nabla \cdot I = 0 \,. \tag{4}$$

3.2.6 Computer simulation

To simulate ITP in a 2-turn S channel, the Nernst-Planck application mode in Comsol Mutiphysics v 3.3 was implemented. A geometry was constructed (Figure 3.3) of a channel with a constant width of 350 μm and an overall length of 2.4 cm. A fixed potential was set at the anode and cathode according to Table 3.1. The insulation/symmetry condition was employed for all other boundaries. The concentration profile of each species was specified for the initial conditions according to Table 3.1, and the initial potential was set to zero. All other species parameters needed for the simulation are given in Table 3.2.

Due to differences in both electric field strength and distance across the width of the separation channel around a turn, dispersion of zones occurs. However, the self-sharpening attribute of ITP allows for the zones to return to a *pseudo* steady-state given a sufficient length of straight channel following a turn. The length required for the zones to return to *pseudo* steady-state, or recovery distance, is obtained by finding the point in a straight channel following a turn where the protein zone has returned to *pseudo* steady-state.

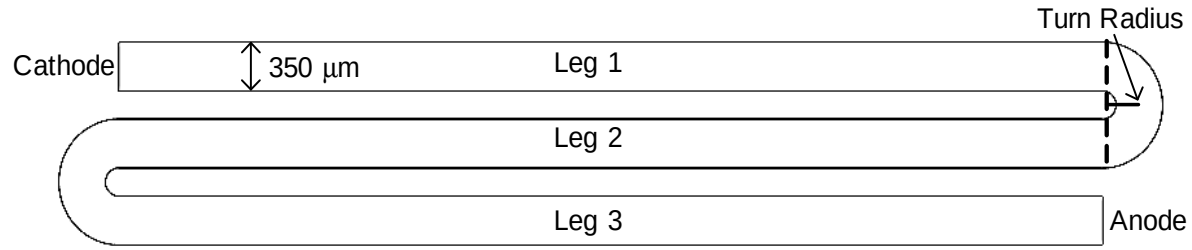

Figure 3.3: Geometry used for ITP simulation. The overall length of the channel is 2.4 cm, and the turn radius is 0.71 channel widths for all simulations, except when turn radius was varied.

Table 3.1: Boundary and initial conditions setup in simulations

	Leading Ion Cl^-	Protein Sample	Terminating Ion EACA	Counter-ion Tris	Voltage
Boundary	Concentration 10 mol/m^3	Concentration 0 mol/m^3	Concentration 0 mol/m^3	Electroneutrality	1000 V[a]
Boundary	Concentration 0 mol/m^3	Concentration 0 mol/m^3	Concentration 60 mol/m^3	Electroneutrality	0 V
All other Boundaries	Insulation	Insulation	Insulation	Insulation	Insulation
Initial Condition Leg 1	Concentration (mol/m^3) $\frac{10}{1+\exp\left[\frac{-2(x-0.0035}{0.0025}\right]^2}$	Concentration (mol/m^3)[b] $0.043\exp\left[\frac{-2(x-0.0035)^2}{0.0025^2}\right]$	Concentration (mol/m^3) $60\exp\left[-\left(\frac{x}{0.0025}\right)^2\right]$	Electroneutrality	0 V
Initial Condition Legs 2, 3	Concentration 10 mol/m^3	Concentration 0 mol/m^3	Concentration 0 mol/m^3	Electroneutrality	0 V

a) Varied during vary voltage simulations

b) Varied during vary concentration simulations

Table 3.2: Parameters of each species used in simulations

	Leading Ion Cl^-	Protein Sample	Terminating Ion EACA	Counter-ion Tris
Absolute Mobility[a]	8.2×10^{-13}	1.34×10^{-14}	2.96×10^{-13}	3.07×10^{-13}
Diffusion Coefficient[b]	2.02×10^{-9}	3.33×10^{-11}	7.31×10^{-10}	7.57×10^{-10}
Charge[c]	-1	-25	-0.14	0.96

a) Absolute mobility, μ_i, (m^2/Vs); Electrophoretic mobility, ω_i, is calculated by $\omega_i = Fz_i\mu_i$

b) Calculated based on Einstein expression: $D_i = \mu_i RT$, units m^2/s

c) Calculated via the Henderson-Hasselbalch equation

This was evaluated using moment analysis to calculate the standard deviation (eqn 5) of the sample zone concentration profile as a function of location in the channel.

$$\sigma = \sqrt{\frac{m_{2x}}{m_{1x}} - \left(\frac{m_{1x}}{m_{0x}}\right)^2 + \frac{m_{2y}}{m_{1y}} - \left(\frac{m_{1y}}{m_{0y}}\right)^2}\,, \tag{5}$$

where m_{nx} and $m_{ny,}$ are the absolute moments obtained by

$$m_{nx} = \int C_p x^n dxdy \tag{6}$$

and

$$m_{ny} = \int C_p y^n dxdy\,, \tag{7}$$

and C_p is the concentration of the protein sample.

In leg two of the channel (Figure 3.1), the zone has reached a *pseudo* steady-state and the standard deviation of the concentration profile is relatively constant. We will call this the *pseudo* steady-state standard deviation (PSSSD). Due to numerical noise, there is a small range of values for the PSSSD, and thus an average PSSSD and 95% confidence interval was calculated for each simulation. As a result of the dispersion of the zone around a turn, the standard deviation of the zone increases as it goes around a turn. As the zone recovers in the straight portion of the channel, the standard deviation returns to its *pseudo* steady-state value. Once the standard deviation of the zone reached the upper limit of the 95% confidence interval of the PSSSD, the zone was considered “recovered”. Recovery distances were measured starting from the beginning of the straight portion of leg 3.

During the simulation, artificial isotropic diffusion was applied to the system to smooth oscillations so that the solution would converge. Isotropic artificial diffusion was set to 0.5 for all simulations. The effect of artificial diffusion built into Comsol Multiphysics varies over the subdomain and is dependent on mesh size and the velocity of species. For this reason, artificial diffusion effects vary as the geometry of the channel or the voltage change.

3.3 Results and Discussion

3.3.1 Experiment

ITP in a two turn S channel was conducted as described above for voltages ranging from 250 V to 4500 V. After applying an electric field, all species began moving towards the anode. Zone formation was observed starting with the trailing end of the Hb zone. The BSA zone formed adjacent to, but in front of the Hb zone. The interfaces between all 4 zones were distinct, however dispersion of zones was observed. In particular, there was a definite cut-off of the concentrated portion of the Hb zone, followed by a "tail" of Hb following the zone (Figure 3.4).

This tail was visible, but much lighter in color than the main Hb band. One cause of this tail may be conductivity gradient instability (CGI) [13, 14]. Above 1500 V CGI was observed as wisps of Hb coming off the back of the main Hb band in a turbulence like fashion (Figure 3.5). These wisps would oscillate in frequency, coming off quickly, then

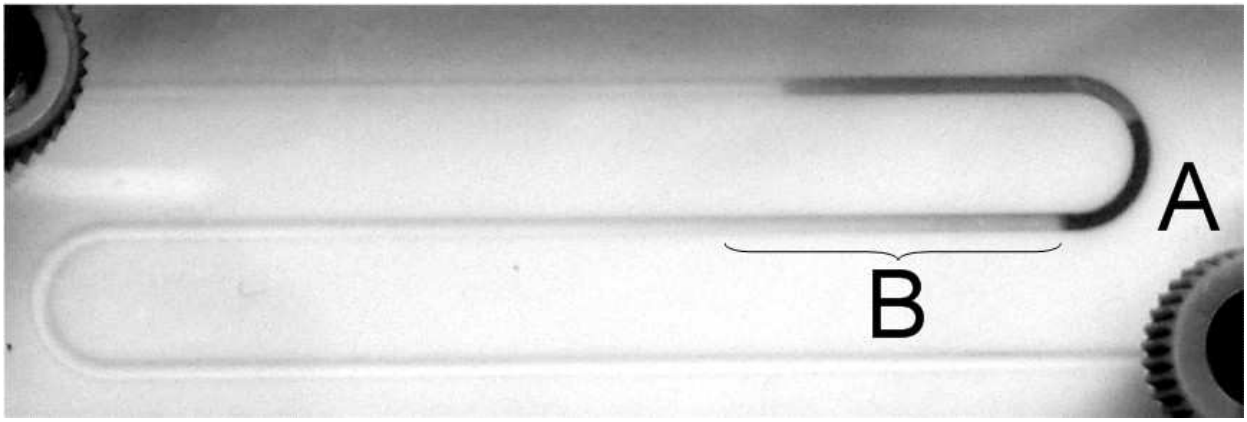

Figure 3.4: Photograph of ITP experiment in S channel. The main Hb band is designated by the letter A, and the Hb tail by B. The zone on the opposite side of the Hb band as the tail is the BSA band.

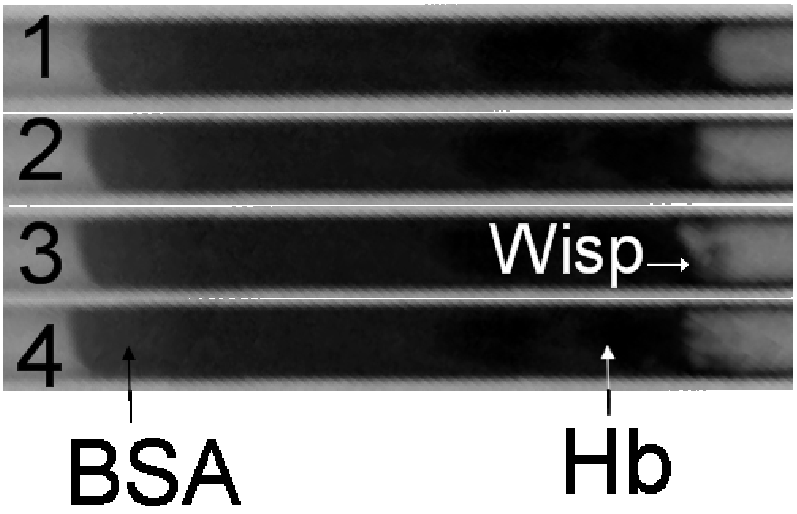

Figure 3.5: Photographs of conductivity gradient instability (CGI) observed during an experiment in an S channel with a constant potential set to 2500 V. The photographs are labeled 1-4, representing a sequence of time. LE was 0.01 M HCl, pH 9.5 and the TE was 0.06 M EACA, pH 10.0. Sample was injected as a 50/50 mix of blue BSA and Hb. Photograph 1 shows the zones at a point where CGI was not observed. Photographs 2-4 show CGI via wisps off the tail end of the Hb zone.

dying down, and cycling. Below 1500 V the wisps attributed to the instability were observed with the aid of a magnifying lamp. As voltage was decreased, the wisps appeared to move slower than they did at higher electric field strengths. At 500 V bands formed, but there was not a clear distinction between the end of the Hb and the TE. Additionally, CGI was not observed at this electric field strength. When the voltage was decreased to 250 V, sharp bands did not form. This indicates that the Hb tail could be due to multiple phenomena, CGI at high electric field strengths, and diffusion at low electric field strengths.

Due to the large turn radius relative to the channel width, the amount of dispersion of the sample zone due to the turns was minimal. For this reason, sample zones returned to *pseudo* steady-state directly after each turn. The minimal dispersion around turns was independent of the voltage applied to the channel.

3.3.2 Modeling

It was desired to characterize the recovery distance for a four component system, containing LE, TE, counter ion, and protein sample. For the system simulated, the ITP zones did not reach *pseudo* steady-state until the zones were into the second leg. Although there was dispersion due to the first turn in the channel, the ITP zones were still able to continue forming while in the turn. This means that although the addition of turns may increase the overall necessary separation length, ITP zones are still maintained.

In the literature on zone electrophoresis in an S channel, the effect of turn radius and turn shape are explored [9, 11, 12]. By increasing the turn radius, it is reported that dispersion caused by a turn decreases. Our modeling of ITP in an S channel showed that due to decreased dispersion around a 180° turn with increased turn radius, the recovery distance decreased as shown in Figure 3.6. The decrease in recovery distance is dramatic for very small turn radii, but levels off as the turn radius passes the width of the column. Figure 3.6 shows a clear trend in the recovery distance even though there is some scatter in the data. This scatter is due to artificial diffusion.

By calculating the recovery distance for three artificial isotropic diffusion values; keeping all other parameters equal, it was found that when the artificial diffusion changes, there is variation in the recovery distance. Since artificial diffusion is linked to geometry mesh and the mesh changes as the turn radius is varied, the effect of artificial diffusion for each turn radius varies, which affects recovery distance.

The effect of voltage on recovery distance was also simulated. Simulations were conducted for voltages ranging from 500 to 3000 V. It was found (Figure 3.7) that the recovery distance was independent of voltage. As voltage is increased the zones move faster, but the distance they must travel to recover does not change.

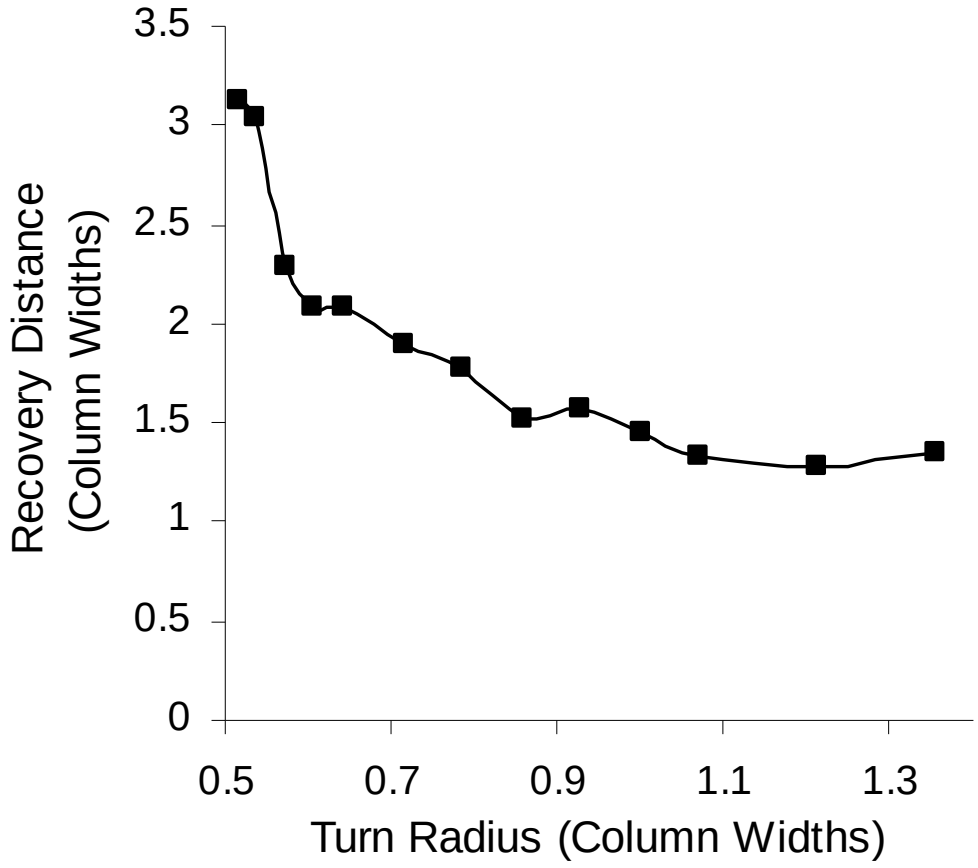

Figure 3.6: Results from simulation of ITP in S channel obtained by calculating the recovery distance for a series of turn radii.

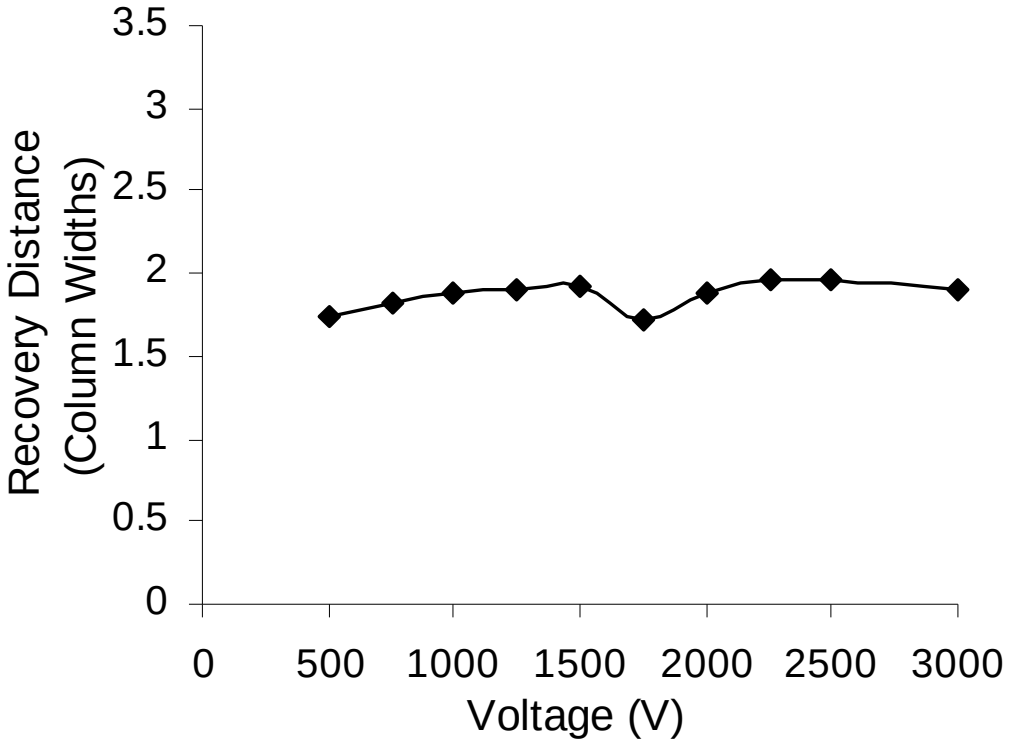

Figure 3.7: Results from simulation of ITP in an S channel for a series of applied voltages.

The effect of sample quantity on recovery distance was studied via changing the initial concentration of protein sample by multiplying by a scalar ranging from 0.25 to 5 times the concentration in Table 3.1. Our results showed that, as the overall mass of sample increases, recovery distance increases. There are two regions of interest in Figure 3.8. The first part of the curve corresponds to sample quantities below that which are required to achieve a plateau concentration. In this region, we see a non-linear increase in recovery distance as sample mass increases. At concentration 2x and above, there is a linear response to increasing the sample quantity. In this region, the sample has reached its plateau concentration, and thus the zone length increases in proportion to sample quantity. Due to the increased sample length, the zone must travel farther to get around the bend, and would naturally require more channel length to recover.

3.4 Concluding Remarks

Our simulation shows that ITP zones are able to recover following a turn in a separation channel and that models can be used to aid in the design of experiments or of apparatuses. One can predict the necessary length of straight channel needed for zones to recover following a turn, or the amount of sample that can be injected into an apparatus to achieve the necessary separation. The model shows that this length is independent of voltage. Our experimental results show that CGI is an issue in a free-flow separation channel for ITP. In order to reduce this phenomenon, the viscosity of the solutions could be raised by an additive such as methyl cellulose. Additionally, the column could be packed with a packing, or filled with a monolith.

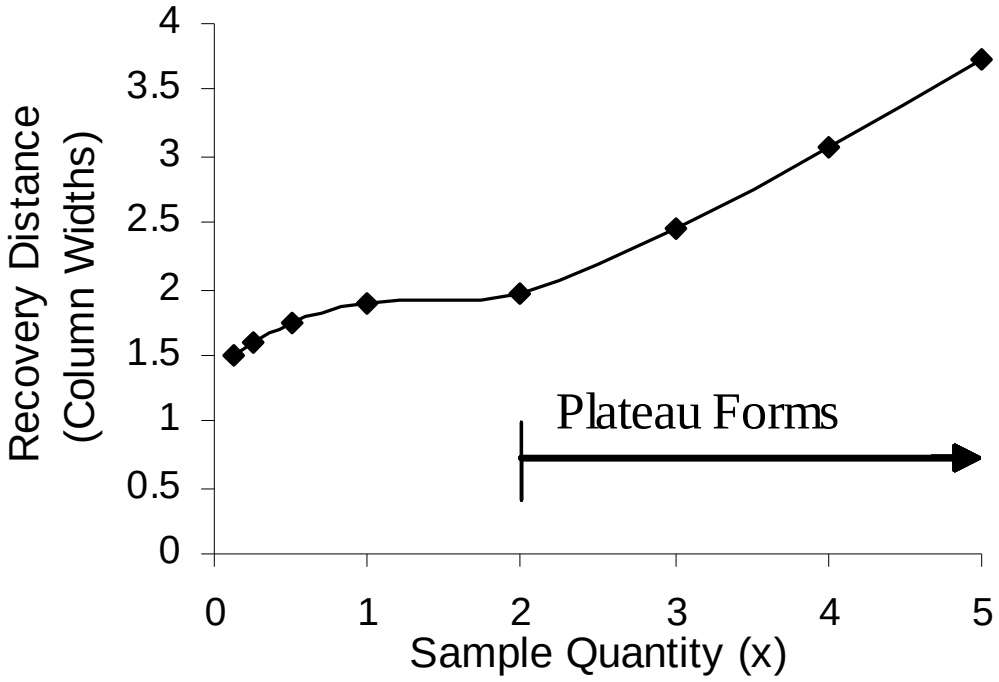

Figure 3.8: Results from simulation of ITP in an S channel for a series of sample masses. Sample masses were varied by changing the initial condition for the protein sample in leg 1. The concentration profile in Table 3.1 represents 1x sample mass, and all other sample masses are a factor of this. Thus to calculate 2x sample mass, the initial concentration profile in Table 1 for the protein species in leg 1 is multiplied by 2.

3.5 Acknowledgements

This material is based upon work supported by the National Institute of General Medical Sciences/National Institutes of Health under Grant No. GM008336, and the Chemical Engineering Department at Washington State University.

3.6 References

[1] Ito, K., Ichihara, T., Zhuo, H., Kumamoto, K., et al., *Analytica Chimica Acta* 2003, *497*, 67-74.

[2] Ölvecká, E., Koníková, M., Grobuschek, N., Kaniansky, D., Stanislawski, B. J., *J. Sep. Sci.* 2003, *26*, 693-700.

[3] Jung, B., Bharadwaj, R., Santiago, J. G., *Anal. Chem.* 2006, *78*, 2319-2327.

[4] Gysler, J., Mazereeuw, M., Helk, B., Heitzmann, M., et al., *J. Chromatogr. A* 1999, *841*, 63-73.

[5] Preetz, W., *Talanta* 1966, *13*, 1649-1660.

[6] Thormann, W., Caslavska, J., Mosher, R. A., *Electrophoresis* 1995, *16*, 2016-2026.

[7] Chen, L., Prest, J. E., Fielden, P. R., Goddard, N. J., Manz, A., Day, P. J. R., *Lab Chip* 2006, *6*, 474-487.

[8] Dolník, V., Liu, S., Jovanovich, S., *Electrophoresis* 2000, *21*, 41-54.

[9] Griffiths, S. K., Nilson, R. H., *Anal. Chem.* 2002, *74*, 2960-2967.

[10] Culbertson, C. T., Jacobson, S. C., Ramsey, J. M., *Anal. Chem.* 1998, *70*, 3781-3789.

[11] Paegel, B. M., Hutt, L. D., Simpson, P. C., Mathies, R. A., *Anal. Chem.* 2000, *72*, 3030-3037.

[12] Griffiths, S. K., Nilson, R. H., *Anal. Chem.* 2001, *73*, 272-278.

[13] Baygents, J. C., Baldessari, F., *Phys. Fluids* 1998, *10*, 301-311.

[14] Lin, H., Storey, B. D., Oddy, M. H., Chen, C., Santiago, J. G., *Phys. Fluids* 2004, *16*, 1922-1935.

CHAPTER FOUR

CONCLUDING REMARKS

This thesis extends the knowledge and prediction of ITP zone behavior in both a preparative scale device, and following turns in a separation channel. In chapter two an analytical expression was derived to predict the location of stationary steady-state zones in a straight channel, under a constant voltage. A comparison of model predictions with results obtained from ITP experiments performed in a vortex stabilized electrophoresis apparatus showed that the model was able to predict the location of immobilized zones within the 95% confidence interval of the experimental data.

The analytical expression presented in chapter two to predict the location of immobilized ITP zones is significant to future experimental design. One application of this predictive tool is for sample detection, either for predicting the necessary placement of a detector for set experimental conditions, or setting the experimental conditions. By controlling the counterflow velocity applied to a system, one can immobilize the sample zone of interest prior to a detector. Once the zone has reached steady-state, and thus its maximum resolution for the specific system, the experimenter can then adjust the counterflow velocity such that the fully formed zone moves past the detector.

The ability to immobilize the ITP train at a specified position within a separation apparatus also allows for continuous operation of a system. By immobilizing the zone of interest at a specified offtake port, one can continuously inject an analyte mixture while withdrawing the target analyte once it has reached a desired concentration. Likewise, for analytes in very low concentration relative to other species in the sample, one can continuously inject the analyte while withdrawing the high abundance species. This concentrates the low abundance species within the channel, while removing contaminating species.

Once a sufficient amount of low abundance species is concentrated within a separation apparatus, it can be removed and injected into a channel with a smaller cross-sectional area to increase resolution. With the reduction in cross-sectional area of a channel, smaller devices are desired. Thus, in order to have sufficient length of channel on a small platform, turns in a channel are introduced. Chapter three describes the simulation and experimental studies of ITP in a two turn separation channel. Simulation showed that dispersion of ITP zones within a bend are observed, however in a straight segment following a turn ITP zones are able to return to *pseudo* steady-state. This is another advantage of ITP over ZE, where zones are unable to recover from the dispersion of zones due to turns. The length of straight segment required for a zone to return to *pseudo* steady-state varies depending on the radius of the turn and the mass of sample; however it is independent of voltage.

The ability to simulate ITP zone behavior in a channel with turns is important to the design of apparatuses and experiments on a small scale. For a given sample mixture, one can design

an apparatus with turns that allows the analytes to achieve *pseudo* steady-state. By varying the geometry in the simulation, one can evaluate the length of straight segment required for various turn radii. In addition, for a specific apparatus, an experimenter can determine the maximum mass of sample that can be injected in order to reach *pseudo* steady-state.

The work presented in this thesis is a foundation for future studies on multi-scale ITP. This work is particularly significant to the area of purification of low abundance species in a sample mixture with a high dynamic range. Immobilization of zones at a specified location allows for a focused analyte to be withdrawn, and then injected into an apparatus with a smaller cross-sectional area. This process can be repeated multiple times from meso to micro and even nano scale. Each time a sample is withdrawn, a portion of the high abundance species is removed, thus allowing for better purity of a low abundance species. Additionally, with each move to a reduced cross-sectional area, better resolution of zones is achieved, further increasing analyte purity. Reducing the cross-sectional area of a separation channel can also increase the concentration of a low abundance species, as was shown in Figure 1.1. This occurs when the cross-sectional area of an apparatus is too large for a mass of sample to achieve a plateau concentration.

Currently at WSU, ITP has been successfully performed from preparative scale, as described in chapter two, down to microchip scale, as described by Cui *et al* [1]. ITP has also successfully been performed intermediate to these scales, as described in chapter three. Future work will involve performing ITP on a model blood system of approximately five

proteins in various concentrations before moving to a real system of approximately 100 species. ITP will first be performed in the vortex stabilized electrophoresis apparatus described in chapter two. Samples containing the analyte of interest will then be combined and injected into the S channel described in chapter three. A sample will then be taken at this scale, and the process will be repeated, moving to decreased cross-sectional areas with each step.

In order successfully take a sample from the S channel previously described, a sample offtake system will need to be implemented into the apparatus. This will likely be achieved via the addition of additional electrodes and legs into the apparatus to direct the zone of interest to a leg of the channel away from the main separation channel. The S channel apparatus will also need to be modified to address the dispersion that was observed during ITP experiments, as described in chapter 3. Dispersion may be decreased by the addition of a packing or monolith into the separation channel.

Additional future work could include the development of a nano scale ITP apparatus. This would allow for an additional step in the multi-scale process. This could be advantageous for very complex sample mixtures with a high dynamic range. In addition, for small sample quantities, the multi-scale process may start at the micro scale, rather than preparative scale, and may require a nano scale apparatus for purification of low abundance species.

4.1 References

1. Cui, H., Dutta, P., Ivory, C. F., Isotachophoresis of proteins in a networked microfluidic chip: Experiment and 2-D simulation. *Electrophoresis* 2007, 28, (7), 1138-1145.